New Journal of Physics
The open access journal at the forefront of physics

Deutsche Physikalische Gesellschaft DPG
IOP Institute of Physics

Published in partnership with: Deutsche Physikalische Gesellschaft and the Institute of Physics

OPEN ACCESS

RECEIVED
6 September 2018

REVISED
1 November 2018

ACCEPTED FOR PUBLICATION
14 November 2018

PUBLISHED
28 February 2019

PAPER

Magnon dressing by orbital excitations in ferromagnetic planes of K_2CuF_4 and $LaMnO_3$

Mateusz Snamina[1] **and Andrzej M Oleś**[2,3]

[1] Kazimierz Gumiński Department of Theoretical Chemistry, Faculty of Chemistry, Jagiellonian University, Gronostajowa 2, PL-30387 Kraków, Poland
[2] Max Planck Institute for Solid State Research, Heisenbergstrasse 1, D-70569 Stuttgart, Germany
[3] Marian Smoluchowski Institute of Physics, Jagiellonian University, Prof. S. Łojasiewicza 11, PL-30348 Kraków, Poland

E-mail: a.m.oles@fkf.mpg.de

Keywords: Mott insulator, magnon dressing, orbital degeneracy, spin-orbital entanglement, spin-orbital superexchange

Abstract

We show that even when spins and orbitals disentangle in the ground state, spin excitations are renormalized by the local tuning of e_g orbitals in ferromagnetic planes of K_2CuF_4 and $LaMnO_3$. As a result, dressed spin excitations (magnons) obtained within the electronic model propagate as quasiparticles and their energy renormalization depends on momentum $\vec{k}$. Therefore magnons in spin-orbital systems go beyond the paradigm of the effective Heisenberg model with nearest neighbor spin exchange derived from the ground state—spin-orbital entanglement in excited states predicts large magnon softening at the Brillouin zone boundary, and in case of $LaMnO_3$ the magnon energy at the $M = (\pi, \pi)$ point may be reduced by ∼45%. In contrast, simultaneously the stiffness constant near the Goldstone mode is almost unaffected. We elucidate physics behind magnon renormalization in spin-orbital systems and explain why long wavelength magnons are unrenormalized while simultaneously energies of short wavelength magnons are reduced by orbital fluctuations. In fact, the $\vec{k}$-dependence of the magnon energy is modified mainly by dispersion which originates from spin exchange between second neighbors along the cubic axes a and b.

1. Introduction

In 3d transition metal compounds strong intraorbital Coulomb interaction U leads to a Mott (or charge-transfer) insulator. Charge excitations between two neighboring 3d ions with m electrons per site, $d_i^m d_j^m \rightleftharpoons d_i^{m+1} d_j^{m-1}$, that occur due to finite kinetic energy $\propto t$, generate superexchange interactions $\propto J = 4t^2/U$ [1]. In their pioneering work Kugel and Khomskii [2] have shown that when degenerate orbitals are partly filled, spin-orbital superexchange couples spin and orbital degrees of freedom. It leads to phases with spin-orbital superexchange in two-dimensional (2D) [3–8] or in three-dimensional (3D) [9–20] systems. When both spin and orbital degrees of freedom are active joint spin-orbital quantum fluctuations arise and may even destabilize long-range order [21]. These fluctuations are the strongest for t_{2g} orbital degrees of freedom [22], where the spin exchange derived from spin-orbital superexchange is strongly entangled and has a dynamical character [23, 24]. In model systems spin-orbital entanglement may be used to identify quantum phase transitions [25].

Orbital degeneracy opens the route towards complex types of spin-orbital order with coexisting antiferromagnetic (AF) and ferromagnetic (FM) exchange bonds. Frequently such systems are analyzed using the classical Goodenough–Kanamori rules [26] which emphasize the complementarity of spin and orbital order, i.e. alternating orbital (AO) order supports FM spin exchange and ferro-orbital order supports AF exchange. They follow from the assumption that spin and orbital excitations are independent of each other and spin exchange interactions may be derived from the spin-orbital superexchange by averaging over the orbital state. Indeed, when joint spin-orbital fluctuations are quenched, e.g. by lattice distortions, these rules apply and the disentangled superexchange helps to understand experimental observations [13]. A good example of this

approach is the parent compound of colossal magnetoresistance manganites $LaMnO_3$ [27], with small spin-orbital entanglement [28]. Therefore, spin waves measured in inelastic neutron scattering [29–31] and optical spectral weights [32] could be successfully interpreted using the effective anisotropic Heisenberg model.

In doped manganites double exchange provides a large FM exchange interaction [27]. It is responsible for the onset of FM order and modifies occupied e_g orbitals involved in the hopping process as demonstrated in the one-dimensional (1D) spin-orbital model [33]. Hole-orbital and orbital-lattice fluctuations were identified as the main origin of the observed unusual softening of the magnon spectrum at the zone boundary [34–36]. It has been shown that orbitons depend thereby on magnons in Mott insulators with orbital degrees of freedom [37–40], and both contribute to spectral properties [41, 42].

In 1D cuprates [43] (2D iridates [44]) orbitons (excitons) are dressed by magnons, while the opposite effect of orbital excitations on magnons was considered only in the context of the strong zone boundary magnon softening observed experimentally in manganites close to half doping [35]. In this paper we demonstrate that spin excitations in a FM plane with AO order, as in K_2CuF_4 [45] or $LaMnO_3$ [46], are indeed renormalized by the changes of occupied e_g orbitals, leading to magnons dressed by orbital fluctuations and propagating together as a quasiparticle in a Mott insulator. This phenomenon is similar to the local changes of AF spin order by an added hole in superconducting cuprates [47].

The remaining of the paper is organized as follows. In section 2 we introduce a general form of spin-orbital Hamiltonian with e_g degrees of freedom and present the magnon excitations starting from orbital order in the ground state. Next we release the constraint of frozen orbitals and present the variational way of finding magnon excitations for optimized orbitals in section 3. A simplified version of this approach and a numerical ansatz (NA) which serves to verify the predictions of the variational approach are presented in section 4. The results for magnons in K_2CuF_4 are given in section 5. We consider a spin excitation in the FM planes of $LaMnO_3$ and analyze the optimal orbital angles near the excitation in section 6. There we also show that the effective spin model will include nearest neighbor J_1, next-nearest neighbor J_2, and third next neighbor J_3 spin exchange, although the spin-orbital superexchange couples only nearest neighbors. Analytic estimation of the renormalized interaction J_1 which determines the magnon bandwidth is presented in the appendix. The paper is concluded with a short summary in section 7.

2. Spin-orbital model and magnons for frozen orbitals

We begin with the e_g orbital basis (labeled in analogy to $|\uparrow\rangle$ and $|\downarrow\rangle$ spin $S=\frac{1}{2}$ states):

$$|\zeta_c\rangle \equiv \frac{1}{\sqrt{6}}(3z^2-r^2), \qquad |\xi_c\rangle \equiv \frac{1}{\sqrt{2}}(x^2-y^2), \tag{1}$$

i.e. a directional orbital $|\zeta_c\rangle$ along the c axis, and an orthogonal to it planar orbital $|\xi_c\rangle$. The energetic splitting of e_g states

$$\hat{H}_z = \frac{1}{2}\sum_i (|\mathrm{i}\zeta_c\rangle\langle \mathrm{i}\zeta_c| - |\mathrm{i}\xi_c\rangle\langle \mathrm{i}\xi_c|) = \sum_i \hat{\tau}_i^{(c)}, \tag{2}$$

selects the favored orbital at site i by the tetragonal crystal field $\propto E_z$. We consider a generic 2D e_g spin-orbital superexchange model on a square lattice

$$\hat{\mathcal{H}} = J(c_1\hat{H}_1 + c_2\hat{H}_2 + c_3\hat{H}_3) + E_z\hat{H}_z, \tag{3}$$

which explains FM order of spins S in the ab planes of K_2CuF_4 $\left(S=\frac{1}{2}\right)$ [48] or $LaMnO_3$ ($S=2$) [10], with three $\{\hat{H}_n\}$ terms explained below. The positive coefficients $\{c_1, c_2, c_3\}$ depend on the multiplet structure of excited $3d^8$ Cu^{3+} states [48] ($3d^5$ Mn^{2+} states [10]) via Hund's exchange J_H/U [13]. In the ground state an e_g hole at a Cu^{2+} ion in K_2CuF_4 (an e_g electron at a Mn^{3+} ion in $LaMnO_3$) occupies a linear combination of two orbital states (1) at site i [1]

$$|\mathrm{i}\vartheta\rangle \equiv \cos(\vartheta/2)|\mathrm{i}\zeta_c\rangle + \sin(\vartheta/2)|\mathrm{i}\xi_c\rangle. \tag{4}$$

When tetragonal distortion is ignored ($E_z=0$), the occupied orbital states on two sublattices A and B are symmetric/antisymmtric combinations of e_g orbital basis $\{|\zeta_c\rangle, |\xi_c\rangle\}$ states with $\vartheta=\pm\pi/2$, otherwise for positive (negative) values of E_z, enhanced amplitude of $|x^2-y^2\rangle$ ($|3z^2-r^2\rangle$) orbital states is favored.

The superexchange part $\propto J$ in equation (3) involves spin $\{\hat{\vec{S}}_i\}$ and orbital pseudospin $\{\hat{\tau}_i^{(\gamma)}\}$ ($\gamma=a,b,c$) operators—it consists of three terms which follow from high-spin ($\hat{H}_1$), low-spin interorbital ($\hat{H}_2$), and low-spin intraorbital ($\hat{H}_3$) charge excitations along nearest neighbor $\langle ij\rangle$ bonds

$$\hat{H}_1 = -\sum_\gamma \sum_{\langle ij\rangle\|\gamma} [\hat{\vec{S}}_i\cdot\hat{\vec{S}}_j + S(S+1)] \otimes \left(\frac{1}{4} - \hat{\tau}_i^{(\gamma)}\hat{\tau}_j^{(\gamma)}\right), \tag{5}$$

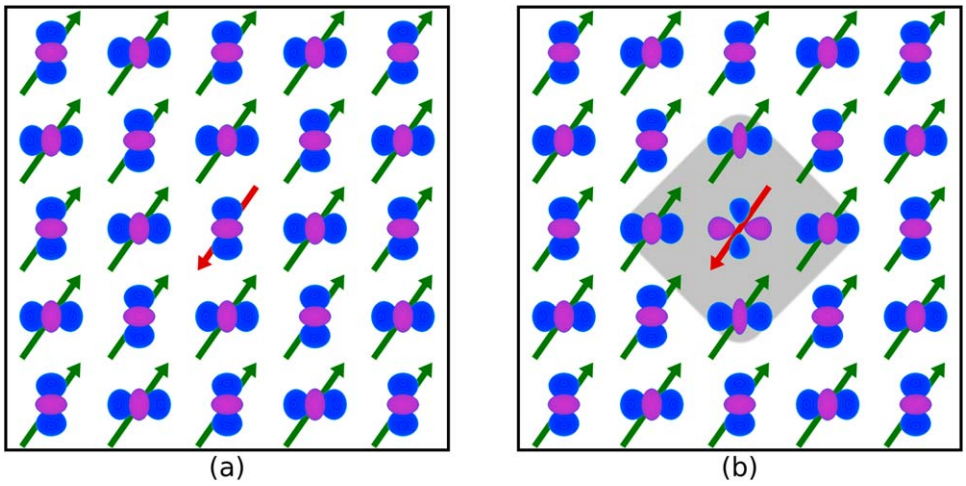

Figure 1. Artist's view of a spin excitation (inverted red arrow) in the FM plane of K_2CuF_4 (green arrows) and AO order (of hole orbitals) at $E_z = -0.8J$, with: (a) frozen orbitals; (b) optimized orbitals at the central spin-flip site itself and at four its neighboring sites in the square lattice, forming a quasiparticle (dressed magnon). The above value of E_z leads to the expected AO order in K_2CuF_4 [50] (different colors indicate the orbital phases), with $\theta_{\rm opt} \simeq 71^\circ$ in equation (4). When the VA is used, case (a) is still realized at $\vec{k} \simeq 0$, while case (b) represents a dressed magnon with $\vec{k} \simeq M$ where orbital states in the shaded cluster are radically different from those in the ground state, see frozen orbitals in (a).

$$\hat{H}_2 = \sum_{\gamma} \sum_{\langle ij \rangle \| \gamma} (\hat{\vec{S}}_i \cdot \hat{\vec{S}}_j - S^2) \otimes \left(\frac{1}{4} - \hat{\tau}_i^{(\gamma)} \hat{\tau}_j^{(\gamma)} \right), \tag{6}$$

$$\hat{H}_3 = \sum_{\gamma} \sum_{\langle ij \rangle \| \gamma} (\hat{\vec{S}}_i \cdot \hat{\vec{S}}_j - S^2) \otimes \left(\frac{1}{2} - \hat{\tau}_i^{(\gamma)} \right) \left(\frac{1}{2} - \hat{\tau}_j^{(\gamma)} \right). \tag{7}$$

The orbital operators $\hat{\tau}_i^{(a)}$ and $\hat{\tau}_i^{(b)}$ for ab planes follow from $\hat{\tau}_i^{(c)}$ along the c axis by a cubic transformation [48], see equation (2).

In K_2CuF_4 one finds FM order at $J_H/U \sim 0.2$ [49], coexisting with AO order [50] of hole orbital states with angles $\pm\theta_{opt}$ on the two sublattices, A and B. Averaging the orbital operators over this AO order in ab planes gives spin Hamiltonian with FM exchange (with $J_\diamondsuit > 0$), $H = -J_\diamondsuit \sum_{\langle ij \rangle} \hat{\vec{S}}_i \cdot \hat{\vec{S}}_j$, which served to interpret the experimental data [51, 52]. To investigate magnons (spin waves) we create a spin excitation at site $i = 0$ by decreasing the value of $S_0^z = S$ to $S_0^z = (S-1)$. In the simplest approach we disentangle [24] spin-orbital superexchange both in the ground and in excited states and use the same frozen AO order shown in figure 1(a) to determine spin exchange $J_\diamondsuit$.

A spin excitation (a magnon) itself is best described by the transformation to Holstein–Primakoff (HP) bosons [53]. In the linear spin-wave theory magnon energy consists of two contributions and we introduce:

(i) Ising energy for a localized HP boson $I^{(0)} \equiv 4J_\diamondsuit S$ and

(ii) the propagating term $P^{(0)}(\vec{k}) \equiv -4J_\diamondsuit S \gamma_{\vec{k}}$.

The latter originates from quantum fluctuations $\propto -\frac{1}{2} J_\diamondsuit (\hat{S}_i^+ \hat{S}_j^- + \hat{S}_i^- \hat{S}_j^+)$, where $\gamma_{\vec{k}} = \frac{1}{4} \sum_{\vec{\delta}} e^{i\vec{k}\cdot\vec{\delta}}$ depends on the momentum $\vec{k} = (k_a, k_b)$ with $k_\alpha \in [-\pi, \pi)$. Here $\vec{\delta}$ stands for one of four nearest neighbors of the central site $i = 0$ shown in figure 1(a). The above two terms determine the magnon dispersion in a 2D ferromagnet,

$$\omega_{\vec{k}}^{(0)} = I^{(0)} + P^{(0)}(\vec{k}) = 4J_\diamondsuit S(1 - \gamma_{\vec{k}}), \tag{8}$$

which serves as a reference below. The breaking of SU(2) symmetry is reflected by a Goldstone mode (at $\vec{k} = 0$), and $\omega_{\vec{k}} = J_\diamondsuit S k^2$ for $\vec{k} \to 0$—we find that this result is insensitive to spin-orbital coupling.

In general however orbitals are not frozen in a spin-orbital system and will respond locally to a spin excitation. One might expect that this reduces spin exchange, $J_\diamondsuit \to J_\blacklozenge$ and the magnon dispersion would soften. Indeed, we have found that the magnon energy $\omega_{\vec{k}}^{(0)}$ is reduced but this effect is rather subtle and the renormalization of exchange interaction $J_\blacklozenge$ depends on momentum $\vec{k}$.

3. Variational approximation

To capture the response of orbital background to a spin excitation we invoke the following variational approximation (VA): significant changes of occupied orbitals with respect to the reference AO order are expected at the nearest neighbors of excited spin and at the site of spin excitation itself, see figure 1(b). The largest change at sublattice $L = A, B$, $\lambda_L(\theta_{\rm opt} + \theta_{1L})$ with $\lambda_A = 1 = -\lambda_B$, occurs at the site of spin excitation itself. For the neighboring sites we use the lattice symmetry and search for the same optimal orbitals given by angles $-\lambda_L(\theta_{\rm opt} + \theta_{2L})$ and $-\lambda_L(\theta_{\rm opt} + \theta_{3L})$ at equivalent neighbors along each cubic axis, a or b.

It is crucial that the VA is performed for each value of momentum $\vec{k}$ independently. We have evaluated the matrix elements of the Hamiltonian $\hat{\mathcal{H}}$ (3) for a single spin excitation in the thermodynamic limit, and determined six variational parameters $\{\theta_{iL}\}$ ($i = 1, 2, 3; L = A, B$). In this way we obtained the renormalized magnon dispersion which replaces equation (8),

$$\omega_{\vec{k}}(\{\theta_{iL}\}) = I(\{\theta_{iL}\}; \vec{k}) + P(\{\theta_{iL}\}; \vec{k}). \tag{9}$$

By construction the angles $\{\theta_{iL}\}$ are real as in equation (4); we have verified that complex coefficients do not lead to further significant energy lowering.

The AO order has a unit cell consisting of two atoms which defines the reduced Brillouin zone (RBZ). The magnon dispersion consists then of two branches in the RBZ, the lower one for $|k_a| + |k_b| \leqslant \pi$, i.e. $\vec{k} \in$ RBZ, and the upper one for vectors $(\vec{k} + \vec{Q}) \notin$ RBZ, where $\vec{Q} = (\pi, \pi)$ is the nesting vector. The two magnon branches give a gapless dispersion and are determined in two steps to take the full advantage of variational parameters. First we find the magnon energies from the lower magnon band—they depend on $I_A(\{\theta_{iA}\}; \vec{k})$, $I_B(\{\theta_{iB}\}; \vec{k})$ and $P_{AB}(\{\theta_{iL}\}; \vec{k})$. The terms $I_L(\{\theta_{iL}\}; \vec{k})$ stand for the Ising HP boson parts, while $P_{AB}(\{\theta_{iL}\}; \vec{k})$ (with $L = a, b$) is obtained from the HP boson propagation along the bonds parallel to the a and b axis, from sublattice A to B (or vice versa).

The eigenstates of the second magnon band are determined in the second step—magnon states which momenta do not belong to the RBZ. As a magnon states with momentum $\vec{k} \notin$ RBZ is orthogonal to its partner magnon state with momentum $(\vec{k} - \vec{Q})$, then, at this stage, the variational principle has to be applied together with rigorous orthogonality condition.

4. Simplified variational approximation (SVA) and NA

Assuming that orbital optimization for both sublattices is equivalent, we use the constraint $\theta_i \equiv \theta_{iA} = \theta_{iB}$ ($i = 1, 2, 3$) which defines SVA. Here we consider the full Brillouin zone and evaluate the energies of a dressed HP boson $I(\{\theta_i\})$ and of its propagating part $P(\{\theta_i\}; \vec{k})$. The SVA is equivalent to the VA when the magnon happens to be a symmetric linear combination of the two waves propagating over the two sublattices—this concerns the $\Gamma - M$ direction; otherwise one may expect that the amplitude of the spin wave is larger in one sublattice and the magnon wave function differs qualitatively from that obtained for a Heisenberg ferromagnet. Below we show that the VA gives indeed better results than the SVA, and the magnon dressing occurs differently on both sublattices.

Finally, we verified the predictions of the VA by exact diagonalization employing a NA with six states per sublattice: a spin defect with or without orbital excitation and four spin-orbital states with spin excitation at the central site together with an orbital excitation at one of nearest neighbors. The state with excitations within a shaded cluster depicted in figure 1(b) may be thus expressed in terms of these six states. Here the constraint for equal orbital angles at two neighbors along the same axis is released. The eigenstates and the spin excitation energy $\omega_{\vec{k}}$ are found separately by exact diagonalization of a 12×12 matrix obtained for each momentum $\vec{k}$.

5. Magnons for K_2CuF_4

Taking as an example the K_2CuF_4 state at $E_z = -0.8J$ shown in figure 1(b), one finds that the orbital renormalization is large—at the central site with spin excitation it is largely modified to $\sim(x^2 - y^2)$ and the orbitals at the four neighboring sites are also changed. The latter orbitals found within the VA are only weakly changed as these latter sites have three neighbors belonging to the neighbors with undisturbed AO order [50], but the one at the spin excitation itself is radically different. For this reason we introduce a cutoff and assume that the orbitals at further neighbors of the excited spin are unchanged. One expects then large dressing of the magnon, with the corresponding reduction of the effective FM interaction to $J_{\blacklozenge}$, particularly in the neighborhood of the M point. This is confirmed by the results shown in figure 2(a)—the magnon energy ω_M is

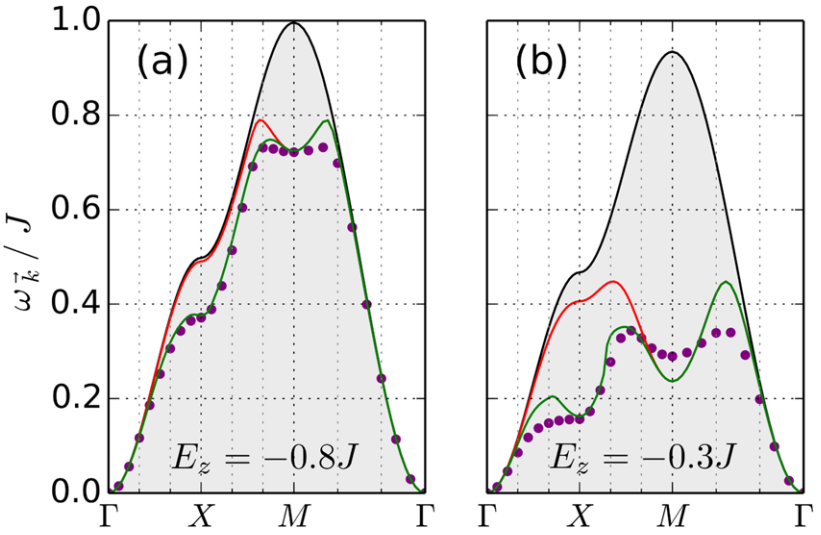

Figure 2. The magnon energy $\omega_{\vec{k}}/J$ obtained for FM state of K_2CuF_4 at $J_H/U = 0.2$ and: (a) $E_z = -0.80J$ and (b) $E_z = -0.30J$. Results are presented for four approximations: frozen orbitals (black line and gray background), the VA (green line), the SVA (red line), and the 12-state NA (purple dots). The high symmetry points are: $\Gamma = (0, 0)$, $X = (\pi, 0)$, $M = (\pi, \pi)$.

reduced by ∼27% from $\omega_M^{(0)}$. Internal consistency of the theory is confirmed by this reduction being nearly the same in all three methods treating spin-orbital coupling: VA, SVA, and NA.

At the X point we recognize the importance of independent optimization of orbitals at the two sublattices—the energy ω_X is reduced by ∼25% from $\omega_X^{(0)}$ in the VA while it stays almost unrenormalized in the SVA, see figure 2(a). The NA agrees very well with the results of the VA except for the points close to the M point along the $M - \Gamma$ path. While the VA may underestimate somewhat the magnon dressing effect, altogether we find indeed a comparison of the VA with the NA very encouraging. The renormalization of magnon energy increases fast when the orbital splitting $|E_z|$ is reduced, and one finds that the magnon energy reduction is large for $E_z = -0.3J$, e.g. by ∼60% at the M point, see figure 2(b). The agreement between the VA and the NA is somewhat worse here but remains still in qualitative agreement. Altogether, we suggest that the magnon softening may be very large for spin-orbital systems with low spin $S = \frac{1}{2}$ as in K_2CuF_4.

6. Magnons for FM planes of $LaMnO_3$

For $LaMnO_3$ we consider electrons in e_g orbitals at $E_z > 0$ and use a representative value of the orbital spitting [54] $E_z = 10c_1J \simeq 1.04J$ which gives $\theta_{\rm opt} \simeq 120^\circ$. Spin and orbital excitations depend on $\theta_{\rm opt}$ for frozen orbitals [55]. The magnon dispersion is modified within the VA or the SVA, see figure 3(a). In agreement with our initial intuition, the magnon energies predicted for dynamical orbitals soften. The energy lowering from $\omega_{\vec{k}}^{(0)}$ to $\omega_{\vec{k}}$ is substantial for this value of E_z—up to about 45% at the M point. We emphasize that the VA and the NA agree almost perfectly and this agreement confirms *a posteriori* our initial choice of real orbital phases in the VA. One observes that the energy $\omega_{\vec{k}}$ is somewhat lower than in the NA in the neighborhood of the M point, indicating that the orbitally doubly excited states become important when at least two orbital deformations are large enough (such states are not included in the NA).

We remark that the reported experimental spin exchange constants are the final product of processing the experimental data concerning the magnons energies. A link between them and the measured energies is established by a parameterized form of the dispersion relation for some conceived pure-spin models defined by a specific interactions pattern. In case of $LaMnO_3$, the simplest Heisenberg model with nearest neighbor interaction J_1 was successfully used to interpret the experimental data in the past [29]—it predicts the magnon dispersion given by equation (8).

We decided to follow the same strategy and studied our *calculated* magnon dispersion $\omega_{\vec{k}}$ in figure 3(a). We tested whether or not one may fit the calculated magnon energies with the effective Heisenberg model and how many exchange interactions are needed using the dispersion $\omega_{\vec{k}}$ discretized over a mesh of (k_a, k_b) values. It turned out that to reproduce the magnon bandwidth $8J_1S$ the fit requires nearest neighbor exchange interaction $J_1 = 6.34 \times 10^{-3}J$, see figure 3(b). Although the reduced value of the magnon bandwidth is then reproduced, the $\vec{k}$-dependence of $\omega_{\vec{k}}$ near the M point is not. It is clear that the Heisenberg model with nearest neighbor exchange is insufficient as the obtained dispersion $\omega_{\vec{k}}$ deviates then from the one derived from the VA, particularly near the M point. The fit may be refined by taking into account the next-nearest and third neighbor interactions, J_2 and J_3, in the effective spin model. One finds that $J_2 = 0.25 \times 10^{-3}J$ is rather small but $J_3 \simeq 1.35 \times 10^{-3}J$ is significant and plays an important role. Both fits are shown in figure 3(b).

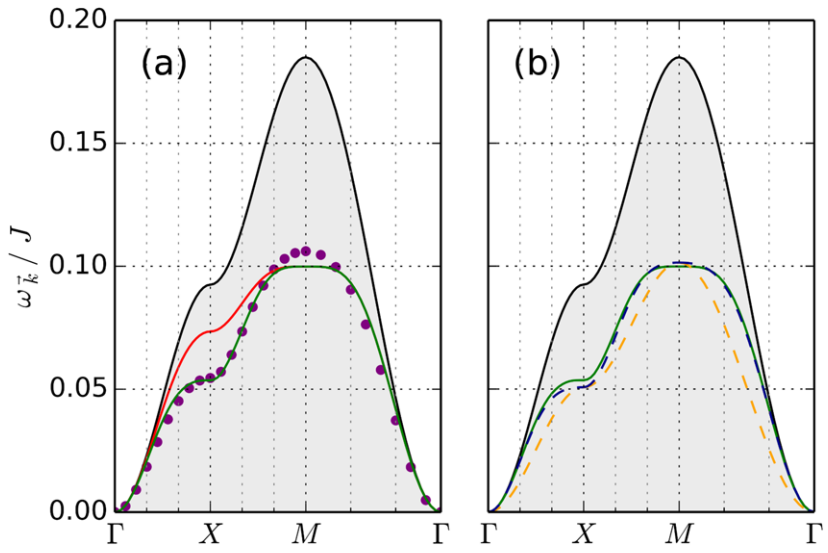

Figure 3. The magnon energy $\omega_{\vec{k}}/J$ for the FM plane of $LaMnO_3$ at $E_z = +1.04J$ obtained: (a) in various approximations, i.e. the *frozen orbital* approach, the VA, and the SVA (black, green, and red line), and the NA (purple dots), and (b) in the VA (green line) and fitted using the Heisenberg model with nearest neighbor $J_1 = 6.34 \times 10^{-3}J$ interaction only (orange line), and with both the above nearest neighbor J_1 and third nearest neighbor $J_3 = 1.35 \times 10^{-3}J$ interactions (dark blue line). Gray shading highlights the difference between the *frozen orbital* approach and the VA. Parameter: $J_H/U = 0.1725$ [10].

The fitted value of the nearest neighbor exchange spin constant $J_1 = 6.34 \times 10^{-3}J$ is much smaller than the value $J_\diamondsuit = 11.56 \times 10^{-3}J$ obtained in the *frozen orbital approach*, actually by $5.22 \times 10^{-3}J$, i.e. by $\sim 0.45J_\diamondsuit$. This reduction of J_1 may be rationalized and was also calculated analytically using our SVA, see the appendix. Expanding the obtained dispersion $\omega_{\vec{k}}$ in the range of small $\vec{k} \to 0$, we derived that

$$J_\diamondsuit \simeq J_1 + 4J_3. \tag{10}$$

This explains why:

(i) the overall magnon bandwidth of $8J_1S$ is here strongly reduced from $\omega_M^{(0)} \simeq 0.185J$ to $\omega_M \simeq 0.101J$, but simultaneously

(ii) the stiffness constant determined by $J_1 + 4J_3$ (by $J_\diamondsuit$ for *frozen orbitals*) remains unrenormalized [56], see equation (10).

We emphasize that in this way an outstanding question in the theory how these two effects may occur simultaneously [34] is explained.

Altogether, the lowering of magnon energy is quite similar for all the methods although some discrepancies occur. We observe that the SVA is here again insufficient when the magnon momentum has large imbalance between its components k_a and k_b. Indeed, for $\vec{k}$ being close to the X point, the SVA is able to give only half of the magnon softening seen in the VA or in the NA, see figure 3. Good agreement between the VA and the NA found here and in K_2CuF_4 at $E_z = -0.8J$ justifies *a posteriori* the idea of independent determination of orbital angles for the sublattices A and B.

The optimal orbital angles $\tilde{\theta}_{iL}$ for a magnon dressed by orbital excitations are changed in $LaMnO_3$ by less than $\pm 30^\circ$ and remain quite similar to the ground state orbitals with $\theta_{\rm opt} = 120^\circ$, see figure 4. In general orbital angles increase for the dressed HP bosons. This may be explained because the optimal values of orbital angles $\tilde{\theta}_{iL}$ follow from the interplay between superexchange interaction and tetragonal crystal field E_z. The first one favors $\theta = 90^\circ$, while the second one favors $\theta = 180^\circ$. When a HP boson is created, the spin exchange effectively decreases while the value of E_z is not affected.

7. Conclusions

Summarizing, we have shown that spin-orbital superexchange tunes the orbital angles near local spin excitations and is responsible for novel dressed magnon quasiparticles. The magnon-orbiton coupling is local and reduces nearest neighbor spin exchange J_1 responsible for magnon dispersion at the M point, while orbital fluctuations couple predominantly to spin excitations at neighboring sites and this generates third nearest neighbor J_3 exchange couplings. Thus spin-orbital entanglement has here similar consequences to the exotic phase suggested as a possible

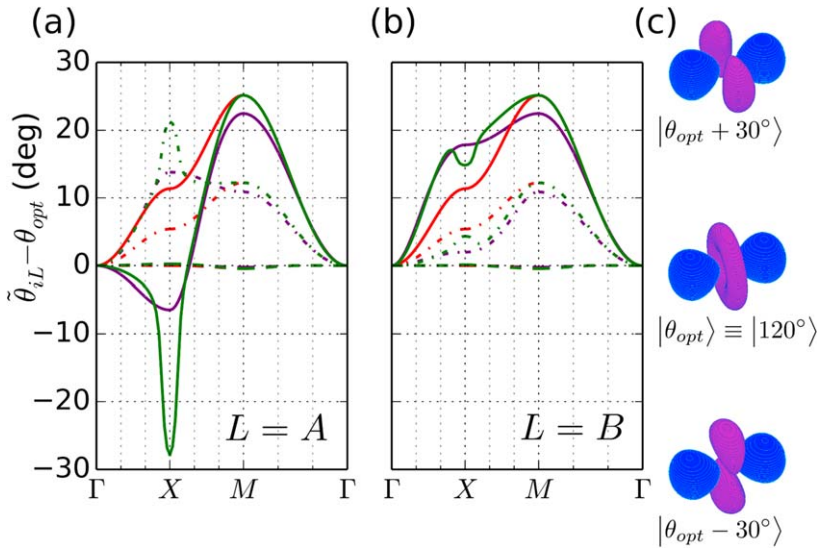

Figure 4. The orbital changes at nearest (solid), next-nearest (dashed), and third nearest neighbor (dotted–dashed lines) of spin excitation in $LaMnO_3$ found in the VA (green), the SVA (red), and the NA (purple lines) for HP bosons at sublattice: (a) *A* and (b) *B*. In (c) orbital states (4) are shown (different colors stand for different orbital phases) for: $\theta_{\rm opt} = 120°$ (middle), $\theta_{iL} = \theta_{\rm opt} - 30°$ (bottom), and $\theta_{iL} = \theta_{\rm opt} + 30°$ (top). Parameters as in figure 3.

ground state of the 2D Kugel–Khomskii model [8]. There the effective spin model derived near a quantum phase transition includes next nearest (J_2) and third nearest (J_3) neighbor exchange interactions and the latter are of crucial importance to stabilize spin orientation. Here spin-orbital entanglement generates also J_3 interactions which couple spins distant by two lattice constants along the cubic axes *a* and *b*, and thus the magnon dispersion is different from that given by the Heisenberg model with nearest neighbor exchange constants derived from frozen orbitals when spin-orbital interactions are disentangled in the ground state. We suggest that such effects would be weaker but still measurable in 3D ordered phases with FM planes, as for instance in $LaMnO_3$, and it is very challenging to detect them.

In the electronic model considered here spin-orbital degrees of freedom are entangled and thus respond jointly, giving renormalized spin excitations. However, strong coupling between orbitals and lattice distortions caused by the Jahn–Teller effect will reduce the magnon-orbiton entanglement and thus the renormalization of magnon dispersion reported here will decrease. We suggest that only future experiments could establish importance of spin-orbital entanglement in excited states.

We suggest that similar analysis of the magnon dispersion could be performed using the variational approach for doped FM manganites with statistically averaged interactions between initial $S = 2$ spins at Mn^{3+} ions and $S = 3/2$ spins at Mn^{4+} ions [57]. We expect that it would reproduce the reduction the magnon energies at the Brillouin zone boundary obtained in the diagrammatic approach [35]. Finally, we remark that the present variational method could also be used to investigate magnon dispersion in the charge, orbital, and spin ordered phase in $La_{1/2}Sr_{3/2}MnO_4$ [58].

Acknowledgments

We thank Wojciech Brzezicki, Krzysztof Rościszewski, Krzysztof Wohlfeld, and particularly Reinhard Kremer and Giniyat Khaliullin for insightful discussions. We kindly acknowledge support by Narodowe Centrum Nauki (NCN, Poland) under Project No. 2016/23/B/ST3/00839. A M Oleś is grateful for the Alexander von Humboldt-Stiftung Fellowship (Humboldt-Forschungspreis).

Appendix. Analytic estimation of the nearest neighbor exchange J_1

Creation of magnons characterized by $\vec{k} = 0$ (being Goldstone modes) does not entail any changes in the orbital background for a spin-orbital system. When magnons characterized by finite $\vec{k} \simeq 0$ are created, the coupled orbitals may be slightly modified. As a result, I and $P(\vec{k})$ terms deviate from $I^{(0)}$ and $P^{(0)}(\vec{k})$. To highlight the minute changes due to spin-orbital entanglement, we introduce a vector $\mathbf{x}$ consisting of differences in variational parameters with respect to their values in the ground state, and expand I and P in terms of $\mathbf{x}$ treated as a small parameter:

$$I(\mathbf{x}) \simeq I^{(0)} + \mathbf{u}^T\mathbf{x} + \frac{1}{2}\mathbf{x}^T\mathbf{U}\mathbf{x}, \tag{11}$$

$$P(\mathbf{x};\vec{k}) \equiv 4T(\mathbf{x})\gamma_{\vec{k}} \simeq P^{(0)}(\vec{k}) + 4\left(\mathbf{w}^T\mathbf{x} + \frac{1}{2}\mathbf{x}^T\mathbf{W}\mathbf{x}\right)\gamma_{\vec{k}}. \tag{12}$$

In the above formulae:

(i) in a considered spin-orbital model (3), the $P(\vec{k})$ term is factorized into the coefficient $4T$ and a $\vec{k}$-dependent term $\gamma_{\vec{k}}$ describing the dispersion;

(ii) for the sake of clarity the following symbols were introduced: **u** and **U** for the gradient and the Hessian of $I(\mathbf{x})$, and **w** and **W** for the gradient and the Hessian of $T(\mathbf{x})$, all at $\mathbf{x} = 0$.

The above expansions were truncated at quadratic terms, so that the corresponding variational function for a magnon energy has a quadratic form

$$\omega_{\vec{k}}(\mathbf{x}) = I(\mathbf{x}) + P(\mathbf{x};\vec{k}) \simeq \omega^{(0)}_{\vec{k}}(\mathbf{x}) + (\mathbf{u}^T + 4\gamma_{\mathbf{k}}\mathbf{w}^T)\mathbf{x} + \frac{1}{2}\mathbf{x}^T(\mathbf{U} + 4\gamma_{\mathbf{k}}\mathbf{W})\mathbf{x}, \tag{13}$$

that may be minimized to obtain

$$\omega_{\vec{k}} \simeq \omega^{(0)}_{\vec{k}} - \frac{1}{2}(\mathbf{u}^T + 4\gamma_{\mathbf{k}}\mathbf{w}^T)(\mathbf{U} + 4\gamma_{\mathbf{k}}\mathbf{W})^{-1}(\mathbf{u} + 4\gamma_{\mathbf{k}}\mathbf{w}). \tag{14}$$

Note that as long as $I(\mathbf{x})$ and $T(\mathbf{x})$ may be expressed analytically, so do **u**, **U**, **w**, **W**, and, finally, $\omega_{\vec{k}}$ as well. Owing to this, the above formula offers analytically the approximate results without involving any further numerical minimization (as opposed to the strategy used in the main part of the article).

If J_1 is perceived as a parameter in a generic form of a dispersion relation $\omega_{\vec{k}} = 4J_1S(1 - \gamma_k) + \ldots$, where all other terms that may be introduced for better accounting of the functional dependence such as $\propto J_3\cos(2k_a)$ are not written explicitly, then its approximate value may be extracted directly from equation (14) as a coefficient in front of $-4S\gamma_k$:

$$J_1^{\mathrm{app}} = J_{\Diamond} + \frac{1}{S}\left(\mathbf{u}^T\mathbf{U}^{-1}\mathbf{w} - \frac{1}{2}\mathbf{u}^T\mathbf{U}^{-1}\mathbf{W}\mathbf{U}^{-1}\mathbf{u}\right), \tag{15}$$

where the second term captures the deviation form the frozen orbital description.

In order to rationalize the reported value of J_1 for $LaMnO_3$ we used equation (15) together with the SVA parametrization. The obtained value of the correction is equal to $J_1^{\mathrm{app}} = -4.90 \times 10^{-3}J$, in fairly good agreement with the value $-5.22 \times 10^{-3}J$ resulting from the fit. To avoid lengthy formulae we do not present here a similar approach to determine J_2 and J_3, and restrict this analytic consideration to the SVA.

ORCID iDs

Andrzej M Oleś https://orcid.org/0000-0002-8954-3233

References

[1] Khomskii D I 2014 *Transition Metal Compounds* (Cambridge: Cambridge University Press)
[2] Kugel K I and Khomskii D I 1973 Crystal structure and magnetic properties of substances with orbital degeneracy *Sov. Phys.—JETP* **37** 725
[3] Vernay F, Penc K, Fazekas P and Mila F 2004 Orbital degeneracy as a source of frustration in $LiNiO_2$ *Phys. Rev.* B **70** 014428
[4] Reitsma A J W, Feiner L F and Oleś A M 2005 Orbital and spin physics in $LiNiO_2$ and $NaNiO_2$ *New J. Phys.* **7** 121
[5] Chaloupka J and Khaliullin G 2008 Orbital order and possible superconductivity in $LaNiO_3/LaMO_3$ superlattices *Phys. Rev. Lett.* **100** 016404
[6] Normand B and Oleś A M 2008 Frustration and entanglement in the t_{2g} spin-orbital model on a triangular lattice: valence-bond and generalized liquid states *Phys. Rev.* B **78** 094427
[7] Corboz P, Läuchli A M, Penc K, Troyer M and Mila F 2011 Simultaneous dimerization and SU(4) symmetry breaking of 4-Color fermions on the square lattice *Phys. Rev. Lett.* **107** 215301
Corboz P, Lajkó M, Läuchli A M, Penc K and Mila F 2012 Spin-orbital quantum liquid on the honeycomb lattice *Phys. Rev.* X **2** 041013
[8] Brzezicki W, Dziarmaga J and Oleś A M 2012 Noncollinear magnetic order stabilized by entangled spin-orbital fluctuations *Phys. Rev. Lett.* **109** 237201
[9] Ishihara S, Yamanaka M and Nagaosa N 1997 Orbital liquid in perovskite transition-metal oxides *Phys. Rev.* B **56** 686
Maezono R, Ishihara S and Nagaosa N 1998 Phase diagram of manganese oxides *Phys. Rev.* B **58** 11583
Okamoto S, Ishihara S and Maekawa S 2002 Orbital ordering in $LaMnO_3$: electron–electron and electron-lattice interactions *Phys. Rev.* B **65** 144403
[10] Feiner L F and Oleś A M 1999 Electronic origin of magnetic and orbital ordering in insulating $LaMnO_3$ *Phys. Rev.* B **59** 3295
[11] Mizokawa T, Khomskii D I and Sawatzky G A 1999 Interplay between orbital ordering and lattice distortions in $LaMnO_3$, YVO_3, and $YTiO_3$ *Phys. Rev.* B **60** 7309

[12] Kim M W, Murugavel P, Parashar S, Lee J S and Noh T W 2004 Origin of the 2 eV peak in optical absorption spectra of $LaMnO_3$: an explanation based on the orbitally degenerate Hubbard model *New J. Phys.* **6** 156
[13] Oleś A M, Khaliullin G, Horsch P and Feiner L F 2005 Fingerprints of spin-orbital physics in cubic Mott insulators: magnetic exchange interactions and optical spectral weights *Phys. Rev.* B **72** 214431
[14] Ishihara S, Murakami Y, Inami T, Ishii K, Mizuki J, Hirota K, Maekawa S and Endoh Y 2005 Theory and experiment of orbital excitations in correlated oxides *New J. Phys.* **7** 119
[15] Zenia H, Gehring G A and Temmerman W M 2005 Orbital ordering in cubic $LaMnO_3$ from first principles calculations *New J. Phys.* **7** 257
[16] Solovyev I V 2008 Spin-orbital superexchange physics emerging from interacting oxygen molecules in KO_2 *New J. Phys.* **10** 013035
[17] Krüger F, Kumar S, Zaanen J and van den Brink J 2009 Spin-orbital frustrations and anomalous metallic state in iron-pnictide superconductors *Phys. Rev.* B **79** 054504
[18] Brzezicki W, Dziarmaga J and Oleś A M 2013 Exotic spin orders driven by orbital fluctuations in the Kugel–Khomskii model *Phys. Rev.* B **87** 064407
[19] Fujioka J, Yamasaki Y, Nakao H, Kumai R, Murakami Y, Nakamura M, Kawasaki M and Tokura Y 2013 Spin-orbital superstructure in strained ferrimagnetic perovskite cobalt oxide *Phys. Rev. Lett.* **111** 027206
[20] Wu Hua 2013 Charge-spin-orbital states in the tri-layered nickelate $La_4Ni_3O_8$: an *ab initio* study *New J. Phys.* **15** 023038
[21] Feiner L F, Oleś A M and Zaanen J 1997 Quantum melting of magnetic order due to orbital fluctuations *Phys. Rev. Lett.* **78** 2799
Feiner L F, Oleś A M and Zaanen J 1998 Quantum disorder versus order-out-of-disorder in the Kugel–Khomskii model *J. Phys.: Condens. Matter* **10** L555
Khaliullin G and Oudovenko V 1997 Spin and orbital excitation spectrum in the Kugel–Khomskii model *Phys. Rev.* B **56** R14243
[22] Khaliullin G 2005 Orbital order and fluctuations in Mott insulator *Prog. Theor. Phys. Suppl.* **160** 155
[23] Oleś A M, Horsch P, Feiner L F and Khaliullin G 2006 Spin-orbital entanglement and violation of the Goodenough–Kanamori rules *Phys. Rev. Lett.* **96** 147205
[24] Oleś A M 2012 Fingerprints of spin-orbital entanglement in transition metal oxides *J. Phys.: Condens. Matter* **24** 313201
Oleś A M 2015 Frustration and entanglement in compass and spin-orbital models *Acta Phys. Polon.* A **127** 163
[25] You W-L, Horsch P and Oleś A M 2015 Entanglement driven phase transitions in spin-orbital models *New J. Phys.* **17** 083009
[26] Goodenough J B 1963 *Magnetism and the Chemical Bond* (New York: Interscience)
[27] Dagotto E, Hotta T and Moreo A 2001 Colossal magnetoresistant materials: the key role of phase separation *Phys. Rep.* **344** 1
Dagotto E 2005 Open questions in cmr manganites, relevance of clustered states and analogies with other compounds including the cuprates *New J. Phys.* **7** 67
[28] Snamina M and Oleś A M 2016 Spin-orbital order in the undoped manganite $LaMnO_3$ at finite temperature *Phys. Rev.* B **94** 214426
[29] Moussa F, Hennion M, Rodríguez-Carvajal J, Moudden M, Pinsard L and Revcolevschi A 1996 Spin waves in the antiferromagnet perovskite $LaMnO_3$: a neutron-scattering study *Phys. Rev.* B **54** 15149
Biotteau G, Hennion M, Moussa F, Rodríguez-Carvajal J, Pinsard L, Revcolevschi A, Mukovskii Y M and Shulyatev D 2001 Approach to the metal-insulator transition in $La_{1-x}Ca_xMnO_3$ ($0 < \sim x < \sim 0.2$): magnetic inhomogeneity and spin-wave anomaly *Phys. Rev.* B **64** 104421
[30] Murakami Y *et al* 1998 Resonant x-ray scattering from orbital ordering in $LaMnO_3$ *Phys. Rev. Lett.* **81** 582
[31] Karpenko B V, Falkovskaya L D and Kuznetsov A V 2008 On the spin wave spectrum in a layered antiferromagnetic structure of the $LaMnO_3$ compound *Phys. Solid State* **50** 2015
[32] Kovaleva N N, Oleś A M, Balbashov A M, Maljuk A, Argyriou D N, Khaliullin G and Keimer B 2010 Low-energy Mott–Hubbard excitations in $LaMnO_3$ probed by optical ellipsometry *Phys. Rev.* B **81** 235130
[33] Daghofer M, Oleś A M and von der Linden W 2004 Orbital polarons versus itinerant e_g electrons in doped manganites *Phys. Rev.* B **70** 184430
[34] Khaliullin G and Kilian R 2000 Theory of anomalous magnon softening in ferromagnetic manganites *Phys. Rev.* B **61** 3494
[35] Singh D K, Kamble B and Singh A 2010 Spin-charge and spin-orbital coupling effects on spin dynamics in ferromagnetic manganites *J. Phys.: Condens. Matter* **22** 396001
Singh D K, Kamble B and Singh A 2010 Orbital fluctuations, spin-orbital coupling, and anomalous magnon softening in an orbitally degenerate ferromagnet *Phys. Rev.* B **81** 064430
[36] Singh D K and Singh A 2013 Magnon self-energy in the correlated ferromagnetic Kondo lattice model: spin-charge coupling effects on magnon excitations in manganites *Phys. Rev.* B **88** 144410
[37] Tanaka Y, Baron A Q R, Kim Y-J, Thomas K J, Hill J P, Honda Z, Iga F, Tsutsui S, Ishikawa D and Nelson C S 2004 Search for orbitons in $LaMnO_3$, $YTiO_3$ and $KCuF_3$ using high-resolution inelastic x-ray scattering *New J. Phys.* **6** 161
[38] Schlappa J *et al* 2012 Spin-orbital separation in the quasi-one-dimensional Mott insulator Sr_2CuO_3 *Nature* **485** 82
[39] Wohlfeld K, Daghofer M, Nishimoto S, Khaliullin G and van den Brink J 2011 Intrinsic coupling of orbital excitations to spin fluctuations in mott insulators *Phys. Rev. Lett.* **107** 147201
Bisogni V *et al* 2015 Orbital control of effective dimensionality: from spin-orbital fractionalization to confinement in the anisotropic ladder system $CaCu_2O_3$ *Phys. Rev. Lett.* **114** 096402
[40] Kim J W, Choi Y, Kim J, Mitchell J F, Jackeli G, Daghofer M, van den Brink J, Khaliullin G and Kim B J 2012 Dimensionality driven spin-flop transition in layered iridates *Phys. Rev. Lett.* **109** 037204
Kim J, Said A H, Casa D, Upton M H, Gog T, Daghofer M, Jackeli G, van den Brink J, Khaliullin G and Kim B J 2012 Large spin-wave energy gap in the bilayer iridate $Sr_3Ir_2O_7$: evidence for enhanced dipolar interactions near the mott metal-insulator transition *Phys. Rev. Lett.* **109** 157402
[41] Ishihara S 2005 Hole dynamics in spin and orbital ordered vanadium perovskites *Phys. Rev. Lett.* **94** 156408
[42] Bieniasz K, Berciu M and Oleś A M 2017 Orbiton-magnon interplay in the spin-orbital polarons of $KCuF_3$ and $LaMnO_3$ *Phys. Rev.* B **95** 235153
[43] Wohlfeld K, Nishimoto S, Haverkort M W and van den Brink J 2013 Microscopic origin of spin-orbital separation in Sr_2CuO_3 *Phys. Rev.* B **88** 195138
[44] Kim J, Daghofer M, Said A H, Gog T, van den Brink J, Khaliullin G and Kim B J 2014 Excitonic quasiparticles in a spin–orbit Mott insulator *Nat. Commun.* **5** 4453
[45] Moreira I P R and Dovesi R 2004 Periodic approach to the electronic structure and magnetic coupling in $KCuF_3$, K_2CuF_4, and $Sr_2CuO_2Cl_2$ low-dimensional magnetic systems *Int. J. Quantum Chem.* **99** 805
[46] Tokura Y 2006 Critical features of colossal magnetoresistive manganites *Rep. Prog. Phys.* **69** 797

[47] Lau B, Berciu M and Sawatzky G A 2011 High-spin polaron in lightly doped CuO_2 *Planes Phys. Rev. Lett.* **106** 036401
Lau B, Berciu M and Sawatzky G A 2011 Computational approach to a doped antiferromagnet: correlations between two spin polarons in the lightly doped CuO_2 plane *Phys. Rev.* B **84** 165102
[48] Oleś A M, Feiner L F and Zaanen J 2000 Quantum melting of magnetic long-range order near orbital degeneracy: classical phases and gaussian fluctuations *Phys. Rev.* B **61** 6257
[49] Onishi T and Yamaguchi K 2008 Theoretical calculations of effective exchange integrals by spin projected and unprojected broken-symmetry methods II: cluster models of Jahn-Teller distorted K_2CuF_4 solid *Polyhedron* **28** 1972
[50] Ito Y and Akimitsu J 1976 Observation of orbital ordering in K_2CuF_4 *J. Phys. Soc. Jpn.* **40** 1333
[51] Moussa F and Villain J 1976 Spin-wave lineshape in two-dimensional K_2CuF_4: neutron experiments and theory *J. Phys. C: Solid State Phys.* **9** 4433
[52] Hirakawa K, Yoshizawa H, Axe J D and Shirane G 1983 Neutron scattering study of spin dynamics at the magnetic phase transition in two-dimensional planar ferromagnet K_2CuF_4 *J. Phys. Soc. Jpn.* **52** 4220
[53] Holstein T and Primakoff H 1940 Field dependence of the intrinsic domain magnetization of a ferromagnet *Phys. Rev.* **58** 1098
[54] Snamina M and Oleś A M 2018 Spin-orbital model of stoichiometric $LaMnO_3$ with tetragonal distortions *Phys. Rev.* B **97** 104417
[55] Bała J, Sawatzky G A, Oleś A M and Macridin A 2001 Quantum decoherence in the spectral functions of undoped $LaMnO_3$ *Phys. Rev. Lett.* **87** 067204
[56] Perring T G, Aeppli G, Hayden M, Carter S A, Remeika J P and Cheong S-W 1996 Spin waves throughout the brillouin zone of a double-exchange ferromagnet *Phys. Rev. Lett.* **77** 711
Fernandez-Baca J A, Dai P, Hwang H Y, Kloc C and Cheong S-W 1998 Evolution of the low-frequency spin dynamics in ferromagnetic manganites *Phys. Rev. Lett.* **80** 4012
[57] Khaliullin G and Kilian R 2000 Theory of anomalous magnon softening in ferromagnetic manganites *Phys. Rev.* B **61** 3494
Oleś A M and Feiner L F 2002 Why spin excitations in metallic ferromagnetic manganites are isotropic *Phys. Rev.* B **65** 052417
[58] Senff D, Krüger F, Scheidl S, Benomar M, Sidis Y, Demmel F and Braden M 2006 Spin-wave dispersion in orbitally ordered $La_{1/2}$ $Mn_{3/2}$ O_4 *Phys. Rev. Lett.* **96** 257201
Johnstone G E, Perring T G, Sikora O, Prabhakaran D and Boothroyd A T 2012 Ground state in a half-doped manganite distinguished by neutron spectroscopy *Phys. Rev. Lett.* **109** 237202